Experimental Confirmation of the General Solution to the Multiple Phase Matching Problem

Alon Bahabad,[†] Noa Voloch,[‡] Ady Arie,[†] and Ron Lifshitz[‡]

[†]*School of Electrical Engineering, Wolfson Faculty of Engineering, Tel Aviv University, Tel Aviv 69978, Israel*
[‡]*School of Physics and Astronomy, Raymond and Beverly Sackler Faculty of Exact Sciences, Tel Aviv University, Tel Aviv 69978, Israel*

Compiled February 6, 2008

We recently described a general solution to the phase matching problem that arises when one wishes to perform an arbitrary number of nonlinear optical processes in a single medium [*Phys. Rev. Lett.* **95**, 133901 (2005)]. Here we outline in detail the implementation of the solution for a one dimensional photonic quasicrystal which acts as a simultaneous frequency doubler for *three* independent optical beams. We confirm this solution experimentally using an electric field poled $KTiOPO_4$ crystal. In optimizing the device, we find—contrary to common practice—that simple duty cycles of 100% and 0% may yield the highest efficiencies, and show that our device is more efficient than a comparable device based on periodic quasi-phase-matching.

OCIS codes: 190.2620, 190.4160, 190.4360.

1. Introduction

Three-wave mixing is a nonlinear optical process that can take place within dielectric materials having a nonlinear $\chi^{(2)}$ coupling coefficient. Such processes are used for a variety of optical frequency conversion applications. Usually, due to dispersion, the three interacting beams do not propagate in phase and so efficient energy transfer between them is prevented.[1] One of the common methods to solve this problem, called quasi-phase-matching (QPM), is to periodically modulate the sign of the relevant component of the nonlinear dielectric tensor at a period corresponding to the phase mismatch.[1,2] This approach is very successful, but unless one is extremely lucky it is limited to the phase matching of a single optical process. In recent years, the need to simultaneously phase match several different processes arose in numerous applications such as creation of multiple radiation sources,[3] of multi-colored solitons,[4] of multi-partite entanglement sources,[5] and for all-optical processing.[6] This need was addressed by developing *ad hoc* generalizations for the quasi-phase-matching procedure, based either on periodic structures in one dimension[7] (for non-collinear processes) and two dimensions[8–10] or specific quasiperiodic structures in one[3,11–14] and two[15] dimensions. In a recent publication [16, henceforth LAB] we explained how to solve the most general problem of multiple phase matching—designing a device to phase match an arbitrary set of processes, defined by any given set of phase-mismatch values. The LAB solution is based on the general observation that the phase matching problem is a consequence of momentum conservation, and that in crystalline matter, *i.e.* matter with long-range order,[17] momentum conservation is replaced with crystal-momentum conservation. Thus, all that one needs to do is to design a nonlinear photonic crystal (NPC)—whether periodic or quasiperiodic—whose Fourier transform is peaked at all the required mismatch wave vectors. Here we present the first experimental realization of a device using this general solution: a one-dimensional three-wave doubler.

Note that other schemes for multiple harmonic generation have been demonstrated before.[12–14] Nevertheless, we choose this relatively simple application of the LAB solution, as it allows us to provide a detailed pedagogical description of the approach. Other than demonstrating that the LAB solution indeed works, we wish to clarify all the steps in the design process, so that others will be able to implement it as well. We stress that the solution is general and is not limited to such simple applications.

2. Simultaneous Phase Matching of Several Interactions

We consider second order nonlinear optical interactions in which three beams couple through the nonlinear susceptibility $\chi^{(2)}$. For a planar process in which two constant undepleted beams, E_1 and E_2, give rise to a third output beam E_3, its integrated field amplitude is given by

$$E_3(\mathbf{\Delta k}) = \Gamma \int_A g(\mathbf{r}) \exp(i\mathbf{\Delta k}\cdot\mathbf{r}) d^2r, \qquad (1)$$

where A is the interaction area, and Γ is a parameter depending on the amplitudes of the incoming waves, on the indices of refraction of all three waves, on the strength of the relevant component of the nonlinear susceptibility tensor d_{ij}, and on the interaction width W. For example, for sum frequency generation in MKS, $\Gamma = \omega_3^2 d_{ij} E_1 E_2 / ic^2 k_3 W$, where c is the speed of light in vacuum. The function $g(\mathbf{r})$ gives the spatial dependence of the relevant nonlinear coupling coefficient, and $\mathbf{\Delta k}$ is the phase mismatch vector of the interacting waves. For sum-frequency generation $\mathbf{\Delta k}$ would be $\mathbf{k}_1 + \mathbf{k}_2 - \mathbf{k}_3$.

It is clear from Eq. (1) that the intensity of the output beam is proportional to the Fourier spectrum of the function $g(\mathbf{r})$, evaluated at the mismatch vector $\mathbf{\Delta k}$.

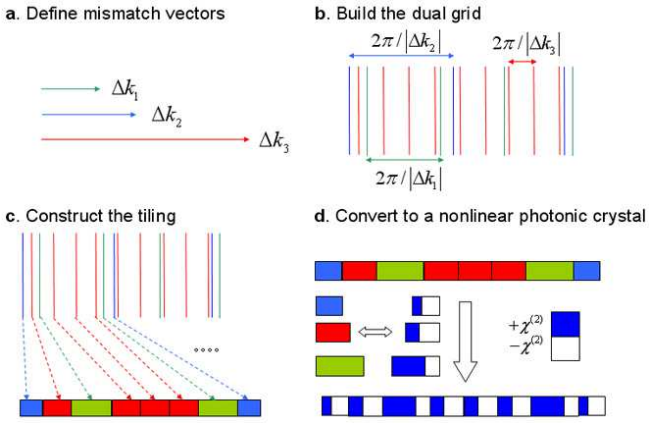

Fig. 1. (Color online) Illustration of the LAB solution for designing a one-dimensional NPC for multiple collinear optical processes, using the dual grid method. (a) The required mismatch vectors. (b) The dual grid, in which each family of lines is shown with a different color. (c) Tiling of the real-space line according to the order in which lines of different families appear in the dual grid. (d) Associating a given duty cycle with each tiling vector. Positively-poled segment are shown in blue, and negatively-poled segments are shown in white.

Thus, if we wish to simultaneously phase-match a set of D three-wave optical precesses, characterized by phase mismatch vectors $\mathbf{\Delta k}^{(j)}$, $j = 1, \ldots D$, we should design the spatial structure of $g(\mathbf{r})$ so that its Fourier spectrum is peaked at all the D mismatch vectors. For a single process, the standard QPM solution[1,2] is to design a one-dimensional NPC with a period of $2\pi/|\Delta k|$, for which there is a first order Bragg peak in the spectrum at $\mathbf{\Delta k}$. The LAB solution shows how to design an appropriate nonlinear photonic crystal—whether periodic or quasiperiodic—such that its spectrum contains Bragg peaks at any given set of D mismatch vectors. The approach that LAB adopt for this purpose is based on the so-called dual-grid method, originally developed by de Bruijn[18] and later generalized[19–21] to become one of the standard methods for creating tiling models of quasicrystals.

The reader in encouraged to consult LAB[16] for a complete and rigorous treatment of the most general two-dimensional multiple phase-matching problem, which we do not repeat here. Instead, we give a detailed demonstration of the LAB solution in one dimension, where all the optical processes are chosen to be collinear. In this case the implementation of the dual-grid method for the design of the NPC, as well as the experimental fabrication of the device, are relatively simple. Nevertheless, we can still design nontrivial and interesting devices, such as the three-wave doubler, implemented here. The basic idea is to find a set of one-dimensional tiling vectors $a^{(i)}$, $i = 1, \ldots D$, with which we can generate a one-dimensional tiling of the line, whereby a tile is simply an interval on the line. We then convert the tiling into an NPC by fabricating whole strips normal to the tiles along the line.

Before starting we wish to point out that in special cases, the D phase mismatch vectors $\mathbf{\Delta k}^{(j)}$ may be integrally dependent. This means that one can use fewer than D wave vectors to generate the NPC and still have Bragg peaks at all D points. It is then a matter of choice whether to use the full set of dependent vectors—although, as pointed out by LAB, it may be difficult in this case to control the intensities of the peaks—or to prefer a smaller set of independent vectors. Here we keep all mismatch vectors and treat them as if they were integrally independent.

3. Designing a One-Dimensional Three-Wave Doubler

We wish to design a device that will simultaneously phase-match three collinear second-harmonic-generation processes, for three different wavelengths in the fiber telecom C-band: $1530nm$, $1550nm$, and $1570nm$. We choose to use the nonlinear crystal $KTiOP_4$ and operate at a temperature of 100°C. At these conditions, the phase-mismatch values for the three processes are:[22,23] $\Delta k^{(1)} = .263\mu m^{-1}$, $\Delta k^{(2)} = .256\mu m^{-1}$, and $\Delta k^{(3)} = .249\mu m^{-1}$ respectively. Thus, we need to design an NPC whose Fourier spectrum contains three collinear wave vectors with these dimensions, as shown schematically in Fig. 1a.

In what follows we describe the design of such a structure, as a particular example of the LAB solution for D collinear processes. Generalizing from $D = 3$ processes to an arbitrary number D of processes, follows directly by replacing all 3-component and 2-component vectors below by D-component and $(D-1)$-component vectors, respectively. Generalizing to higher dimensional processes requires use of the full solution, as described by LAB.

A. *Finding the tiling vectors*

To calculate the corresponding three collinear tiling vectors, $a^{(i)}$, $i = 1, \ldots 3$, we first construct a single three-component vector $\mathbf{k}_1 = (\Delta k^{(1)}, \Delta k^{(2)}, \Delta k^{(3)})$ from the three given mismatch values. This vector spans a one-dimensional subspace of an abstract three-dimensional vector space. We complete it to an orthogonal basis of the three-dimensional space by adding two orthogonal vectors $\mathbf{q}_2$ and $\mathbf{q}_3$. These are, of course, not unique, and we choose them to be $\mathbf{q}_2 = (0.6483, -0.3421, -0.3331)$ and $\mathbf{q}_3 = (-0.3421, 0.6672, -0.3240)$. We use these three vectors as the columns of a 3×3 non-singular matrix,

$$\begin{pmatrix} \mathbf{K}^{(1)} \\ \mathbf{K}^{(2)} \\ \mathbf{K}^{(3)} \end{pmatrix} \equiv \begin{pmatrix} \Delta k^{(1)} & q_2^{(1)} & q_3^{(1)} \\ \Delta k^{(2)} & q_2^{(2)} & q_3^{(2)} \\ \Delta k^{(3)} & q_2^{(3)} & q_3^{(3)} \end{pmatrix}, \qquad (2)$$

whose rows $\mathbf{K}^{(j)}$, $j = 1, \ldots 3$, span the three-dimensional vector space as well. We then find the three dual basis

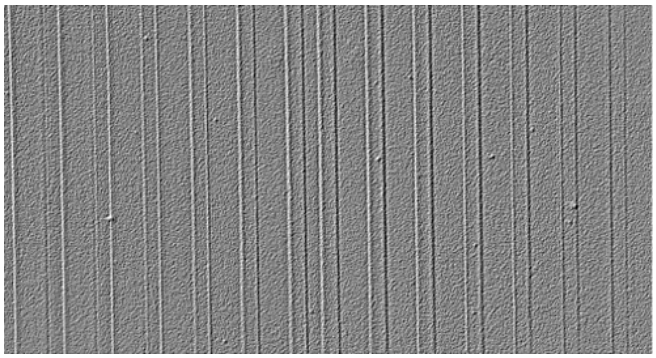

Fig. 2. An optical microscope image of the demonstrated NPC. The prominent elements correspond to the $a^{(1)}$ tiling vector, poled with a 100% duty cycle. Their width is $8.5\mu m$. The distances between these elements are quasiperiodically ordered along with the $a^{(2)}$ and $a^{(3)}$ tiling vectors, whose widths are $8.1\mu m$ and $7.9\mu m$, respectively, and which are poled with a 0% duty cycle.

vectors, denoted

$$\begin{pmatrix} \mathbf{A}^{(1)} \\ \mathbf{A}^{(2)} \\ \mathbf{A}^{(3)} \end{pmatrix} \equiv \begin{pmatrix} a^{(1)} & b_2^{(1)} & b_3^{(1)} \\ a^{(2)} & b_2^{(2)} & b_3^{(2)} \\ a^{(3)} & b_2^{(3)} & b_3^{(3)} \end{pmatrix}, \tag{3}$$

by solving the three-dimensional orthogonality relations

$$\mathbf{A}^{(i)} \cdot \mathbf{K}^{(j)} = 2\pi\delta_{ij}. \tag{4}$$

Each row of the matrix (3) is a dual-basis vector of the form $\mathbf{A}^{(j)} = (a^{(j)}, \mathbf{b}^{(j)})$. The $a^{(j)}$ are the three required collinear tiling vectors, whose values are calculated to be $a^{(1)} = 8.3946\mu m$, $a^{(2)} = 8.1652\mu m$, and $a^{(3)} = 7.95\mu m$. The 2-dimensional vectors $\mathbf{b}^{(j)}$ can be used, as explained by LAB, to analytically calculate the Fourier transform of the NPC in order to determine the expected efficiencies for the different nonlinear processes.

B. Constructing the tiling

If we were now asked to generate all points at integral linear combinations of the three tiling vectors we would get the unwanted outcome of a dense filling of the real line. To avoid this situation we construct the dual grid, whose topology determines which of the integral linear combination of the tiling vectors are to be included in the one-dimensional tiling.

The dual grid is constructed by associating with each mismatch vector $\Delta k^{(j)}$, $j = 1, \ldots 3$, an infinite family of parallel lines separated by a distance $L_j = 2\pi/\Delta k^{(j)}$, as illustrated in Fig. 1b. The set of all families together constitutes the dual grid. We use the freedom to shift each family from the origin by an arbitrary value of $f_j L_j$, where $0 \leq f_j < 1$, so that lines from different families never exactly coincide. Because the mismatch vectors are independent over the integers, such a shift produces a so-called gauge-transformation[20,21] which has no effect on the resulting NPC.

The rest follows immediately, as the required order of the tiles in the real-space structure is given by the order in which lines of different families appear in the dual grid. This is illustrated in Fig. 1c. This is the sense in which the topology of the dual grid determines the real-space tiling in this trivial one-dimensional setting. The duality is a statement that each line in the grid is associated with a tile, or interval, in the tiling; and each interval in the grid with a vertex of the tiling. In our example, approximately 800 lines are required in each family to generate a $1cm$ long one-dimensional nonlinear photonic quasicrystal.

C. Building a nonlinear photonic crystal from the tiling

To create an actual nonlinear photonic quasicrystal we modulate the relevant component of the nonlinear susceptibility tensor $\chi^{(2)}$ according to the constructed tiling. Technology usually permits us to use a binary modulation of $\chi^{(2)}$ so that the actual crystal can be represented by a normalized function $g(r) = \pm 1$. The simplest representation from a theoretical standpoint would be to attach a thin strip of value $g(r) = 1$ to every vertex of the tiling, while assigning the background a value of $g(r) = -1$. This is equivalent to a simple convolution of the strip with delta functions at the vertices of the tiling, and therefore gives the simplest analytical expression for the Fourier transform of the function $g(r)$.[16] Nevertheless, it does not necessarily produce an optimal NPC—one in which the strongest Bragg peaks are associated with the three mismatch vectors. In general, one can use a numerical procedure in order to optimize the required Bragg peaks. See for example the treatment by Norton and de Sterke.[24] Here we want to give a few quick-and-simple solutions—in addition to the thin strips—that are worth trying if one does not wish to deal with numerical optimization.

A second option would be to use strips whose widths are equal to the tile vectors and simply to change the sign of $g(r)$ from one strip to the next. In this way, exactly half the tiles will give strips of value $g(r) = 1$, and the other half strips of value $g(r) = -1$. The generated set of strips would be analogous to an antiferromagnetic quasicrystal,[25,26] whose Fourier transform could also be calculated analytically. We have found that this option does not yield an optimal NPC for this application.

A third option, and the one which we actually implemented, is again to use strips whose widths are equal to the tile vectors, but this time associate a so-called duty cycle with each tiling vector. This is done by dividing each tiling vector into two segments, and assigning a value of $g(r) = 1$ to one segment, and $g(r) = -1$ to the other. The duty cycle is the fraction of each strip with $g(r) = 1$. This general procedure is shown schematically in Fig. 1d. It gives us the ability to perform simple spectral shaping. By varying the three duty cycles, associated with the three tiling vectors, we can engineer the magnitudes of the Fourier coefficients of the three required Bragg peaks. What we actually find—contrary

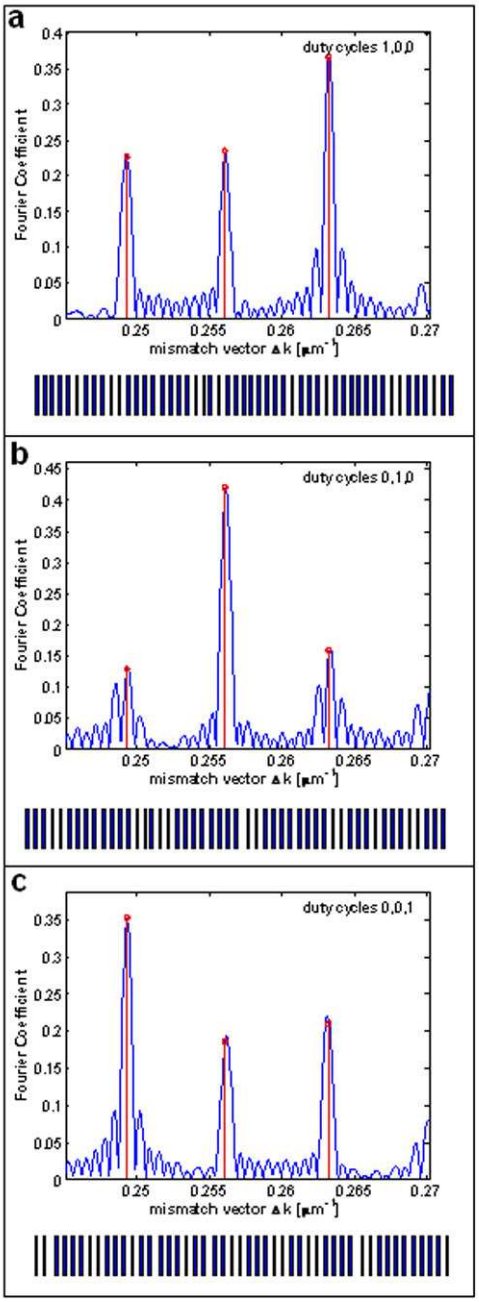

Fig. 3. (Color online) Spectral shaping. Each panel shows the magnitude of the Fourier transform for a $1cm$ long NPC made to phase match the three collinear processes, described in the text. In each panel one of the tiling vectors is given a duty cycle of 100%, denoted as 1, and the remaining two a duty cycle of 0%, or 0. Each panel also shows a piece of the corresponding real-space representation of the NPC, where the smallest element size is $8\mu m$.

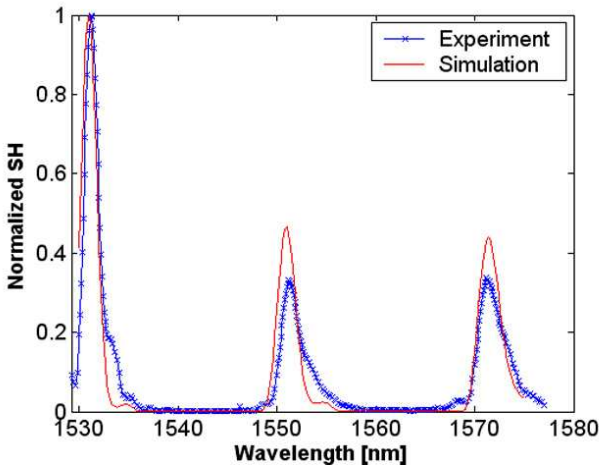

Fig. 4. (Color online) Normalized pump wavelength response. Experiment and simulation results of second harmonic generation as a function of pump wavelength. This figure corresponds to panel (a) of Fig. 3.

to common practice[3,11,27]—is that the optimal NPC's are obtained when we use duty cycles of either 100% or 0%. These are also easiest to fabricate in terms of the required resolution as we associate a value of $g(r) = 1$ or $g(r) = -1$ to tiles as a whole.

In the experimental image of the NPC, shown in Fig. 2, the tiling vector $a^{(1)}$ is associated with strips of value $g(r) = 1$, or a duty cycle of 100%, while the other two have a value of $g(r) = -1$, or a duty cycle of 0%. In Fig. 3 we show numerical calculations of the magnitude of the Fourier transform of $g(r)$, for the three possible assignments of a value of $g(r) = 1$ to one tiling vector, and a value of $g(r) = -1$ to the other two. One clearly sees that in all cases there are pronounced Bragg peaks exactly where we want them to be, but the distribution of intensities changes as we vary the tiling vector that is assigned a 100% duty cycle. The magnitudes of the Fourier coefficients are comparable to the $2/\pi \simeq 0.6366$ figure of merit, which is the magnitude of the first order Fourier component for a one-dimensional periodic NPC. In fact, because the efficiency is measured in terms of energy transfer it depends on the Fourier intensity and on the square of the interaction length. Thus, the real comparison should be with the efficiency per process of a sequence of three periodic NPC's, each of length $L/3$, which is proportional to $\left(\frac{1}{3}\cdot\frac{2}{\pi}\right)^2 = 0.045$. For the homogeneous nonlinear photonic quasicrystal that we implement here the lowest process efficiency is proportional to $(1\cdot 0.23)^2 = 0.053$ and the highest to $(1\cdot 0.365)^2 = 0.133$, both better than the composite periodic structure.

The ability to shape the spectrum using different representation of the function $g(r)$ can be very useful for cascaded processes that to some extent are better performed in sequence. For example, in multi-harmonic generation, where the outputs of some of the processes serve as inputs for others, it might be beneficial to give prece-

Table 1. Conversion efficiencies. Maximum conversion efficiencies are obtained for the indicated wavelengths. In the simulation, the maximum efficiency of the third process was shifted by $+0.4nm$.

Wavelength	Experimental efficiency [1/Watt]	Theoretical efficiency [1/Watt]	Simulated efficiency [1/Watt]
$1531nm$	1.19e-3	1.5e-3	1.46e-3
$1551nm$	3.37e-4	6.13e-4	6.83e-4
$1571nm$	3.18e-4	5.49e-4	6.43e-4

dence to the efficiencies of the initial processes at the beginning of the NPC and gradually, along the interaction length, change the balance in favor of the latter processes.

4. Experimental Results

The NPC was fabricated by electric field poling[28] of $KTiOPO_4$, and is shown in Fig. 2. The spatial modulation was performed along $1cm$ with a $2\times1mm^2$ cross section. To test the NPC we used a pump beam from a tunable external cavity diode laser, followed by an Erbium-doped fiber amplifier, and a fiber polarization controller whose purpose is to polarize the beam to be perpendicular to the plane of modulation of the NPC. The pump beam was then chopped at a frequency of 1kHz and focused to a waist of $20\mu m$ in the middle of the crystal. Its power was varied during the experiment in the range of $4-40mW$. The NPC was kept at a constant temperature of 100°C. The input pump wavelength was varied in the range $1528nm-1577nm$ and the resulting second harmonic power was measured using a calibrated Silicon photo-diode, followed by a lock-in amplifier. The results were compared with a simulation employing a split step Fourier method,[29] in which a non-depleted Gaussian beam was used as a pump. Both results exhibit excellent agreement, as can be seen in Fig. 4, and show that this device is indeed most efficient for second harmonic generation of the three designated pump wavelengths.

Note that for focused Gaussian beams[30] the actual peak efficiencies are shifted by $1nm$ towards longer wavelengths, as compared to the idealized design using plane wave interaction. However, with temperature tuning the results can be shifted in both directions. For the wavelength range used here, the shift rate is $0.1nm$ per degree centigrade. The conversion efficiencies were also calculated theoretically using the Boyd-Kleinman formalism for focused Gaussian beams, propagating within a homogeneous nonlinear crystal,[30] modified to include the relevant Fourier coefficient. The nonlinear conversion efficiencies for the wavelengths for which conversion was maximal are shown in Table 1. The small discrepancies between theory and simulation are attributed to the assumption, made in the theoretical calculation, that each processes is affected only by its relevant Fourier component. In the simulation the propagating waves experience small but still non-negligible contributions from close-by spectral components.

5. Summary

We present the first experimental realization of a nonlinear optical device employing the general solution of the phase matching problem, given by LAB. The demonstrated device is a one-dimensional three-wave doubler. We show that by simply using 100% or 0% duty cycles, each of the three wave doubling processes exhibits high efficiency. Moreover, the efficiencies are all higher than for a device employing a periodic modulation with the same overall interaction length. We demonstrate the ability to perform spectral shaping of the response by changing the duty cycles, associated with the different tiles. This allows us to strengthen certain processes at the expense of others. It should be stressed once more that the LAB solution is general and can support any set of nonlinear processes, not only for one-dimensional problems but also in two or three dimensions, without any symmetry restrictions. In addition, this general method can be applied to a broad range of problems from generation of radiation sources through all-optical processing to generation of entangled photons in quantum optics applications.

6. Acknowledgments

This research is supported by the Israel Science Foundation through grants no. 960/05 and 684/06.

References

1. J. A. Armstrong, N. Bloembergen, J. Ducuing, and P. S. Pershan, "Interactions between Light Waves in a Nonlinear Dielectric," Physical Review **127**, 1918–1939 (1962).
2. M. M. Fejer, G. A. Magel, D. H. Jundt, and R. L. Byer, "Quasi-phase-matched second harmonic generation - Tuning and tolerances," IEEE Journal of Quantum Electronics **28**, 2631–2654 (1992).
3. S.-N. Zhu, Y.-Y. Zhu, and N.-B. Ming, "Quasi-Phase-Matched Third-Harmonic Generation in a Quasi-Periodic Optical Superlattice," Science **278**, 843 (1997).
4. Y. S. Kivshar, A. A. Sukhorukov, and S. M. Saltiel, "Two-color multistep cascading and parametric soliton-induced waveguides," Phys. Rev. E **60**(5), R5056–R5059 (1999).
5. R. C. Pooser and O. Pfister, "Observation of triply coincident nonlinearities in periodically poled $KTiOPO_4$," Opt. Lett. **30**, 2635–2637 (2005).
6. G. I. Stegeman, D. J. Hagan, and L. Torner, "$\chi^{(2)}$ cascading phenomena and their applications to all-optical signal processing, mode-locking, pulse compres-

sion and solitons," Opt. Quantum Electron. **28**, 1691–1740 (1996).
7. T. Ellenbogen, A. Arie, and S. M. Saltiel, "Non-collinear double quasi phase matching in one dimensional poled crystals," Optics Letters (to be published).
8. V. Berger, "Nonlinear Photonic Crystals," Phys. Rev. Lett. **81**(19), 4136–4139 (1998).
9. N. G. R. Broderick, G. W. Ross, H. L. Offerhaus, D. J. Richardson, and D. C. Hanna, "Hexagonally Poled Lithium Niobate: A Two-Dimensional Nonlinear Photonic Crystal," Phys. Rev. Lett. **84**(19), 4345–4348 (2000).
10. A. Arie, N. Habshoosh, and A. Bahabad, "Quasi phase matching in two-dimensional nonlinear photonic crystals," Optical and Quantum Electronics (to be published).
11. K. Fradkin-Kashi, A. Arie, P. Urenski, and G. Rosenman, "Multiple Nonlinear Optical Interactions with Arbitrary Wave Vector Differences," Phys. Rev. Lett. **88**(2), 023903 (2001).
12. H. Liu, S. N. Zhu, Y. Y. Zhu, N. B. Ming, X. C. Lin, W. J. Ling, A. Y. Yao, and Z. Y. Xu, "Multiple-wavelength second-harmonic generation in aperiodic optical superlattices," Applied Physics Letters **81**, 3326–3328 (2002).
13. J. Liao, J. L. He, H. Liu, J. Du, F. Xu, H. T. Wang, S. N. Zhu, Y. Y. Zhu, and N. B. Ming, "Red, yellow, green and blue - four-color light from a single, aperiodically poled $LiTaO_3$ crystal," Applied Physics B: Lasers and Optics **78**, 265–267 (2004).
14. M. H. Chou, K. R. Parameswaran, M. M. Fejer, and I. Brener, "Multiple-channel wavelengthconversion by use of engineered quasi-phase-matching structures in $LiNbO_3$ waveguides," Optics Letters **24**, 1157–1159 (1999).
15. R. T. Bratfalean, A. C. Peacock, N. G. R. Broderick, K. Gallo, and R. Lewen, "Harmonic generation in a two-dimensional nonlinear quasi-crystal," Optics Letters **30**, 424–426 (2005).
16. R. Lifshitz, A. Arie, and A. Bahabad, "Photonic Quasicrystals for Nonlinear Optical Frequency Conversion," Physical Review Letters **95**(13), 133901 (2005).
17. R. Lifshitz, "What is a crystal?" Preprint (cond-mat/0701029).
18. N. de Bruijn, "Algebraic theory of Penrose's non-periodic tilings of the plane," Proc. K. Ned. Akad. Wet., Ser. A **84**, 39–66 (1981).
19. F. Gahler and J. Rhyner, "Equivalence of the generalised grid and projection methods for the construction of quasiperiodic tilings ," Journal of Physics A Mathematical General **19**, 267–277 (1986).
20. D. A. Rabson, T.-L. Ho, and N. D. Mermin, "Aperiodic tilings with non-symmorphic space groups $p2^j gm$," Acta Crystallographica Section A **44**(5), 678–688 (1988). URL `http://dx.doi.org/10.1107/S0108767388003733`.
21. D. A. Rabson, T.-L. Ho, and N. D. Mermin, "Space groups of quasicrystallographic tilings," Acta Crystallographica Section A **45**(8), 538–547 (1989). URL `http://dx.doi.org/10.1107/S0108767389003302`.
22. K. Fradkin, A. Arie, A. Skliar, and G. Rosenman, "Tunable midinfrared source by difference frequency generation in bulk periodically poled $KTiOPO_4$," Applied Physics Letters **74**, 914–916 (1999).
23. S. Emanueli and A. Arie, "Temperature-dependent dispersion equations for $KTiOPO_4$ and $KTiOAsO_4$," Appl. Opt. **42**, 6661–6665 (2003).
24. A. H. Norton and C. M. de Sterke, "Optimal poling of nonlinear photonic crystals for frequency conversion," Optics Letters **28**, 188–190 (2003).
25. R. Lifshitz, "Symmetry of Magnetically Ordered Quasicrystals," Phys. Rev. Lett. **80**(12), 2717–2720 (1998).
26. R. Lifshitz, "Magnetic quasicrystals: What can we expect to see in their neutron diffraction data?" Materials Science and Engineering A **294**, 508–511 (2000).
27. K. Fradkin-Kashi and A. Arie, "Multiple-wavelength quasi-phase-matched nonlinear interactions," IEEE J. Quantum Electron **35**, 1649–1656 (1999).
28. M. Yamada, N. Nada, M. Saitoh, and K. Watanabe, "First-order quasi-phase matched $LiNbO_3$ waveguide periodically poled by applying an external field for efficient blue second-harmonic generation," Applied Physics Letters **62**, 435–436 (1993).
29. G. P. Agrawal, *Nonlinear Fiber Optics* (Academic Press, 2001).
30. G. D. Boyd and D. A. Kleinman, "Parametric interaction of focused Gaussian light beams," J. Appl. Phys. **39**, 3596–3639 (1968).